Evaluation of Different Dielectric Barrier Discharge Plasma Configurations As an Alternative Technology for Green C_1 Chemistry in the Carbon Dioxide Reforming of Methane and the Direct Decomposition of Methanol†

Víctor J. Rico,‡ José L. Hueso,*,‡,§,⊥ José Cotrino,‡,|| and Agustín R. González-Elipe‡

Instituto de Ciencia de Materiales de Sevilla (CSIC-Universidad de Sevilla), Departamento de Química Inorgánica, Universidad de Sevilla, Spain, Departamento de Física Atómica, Molecular y Nuclear, Universidad de Sevilla, Spain

Received: January 13, 2010; Revised Manuscript Received: February 4, 2010

Carbon dioxide reforming of methane and direct decomposition of methanol have been investigated using dielectric barrier discharges (DBD) at atmospheric pressure and reduced working temperatures. Two different plasma reactor configurations are compared and especial attention is paid to the influence of the surface roughness of the electrodes on the conversion yields in the first plasma device. The influence of different filling gap dielectric materials (i.e., Al_2O_3 or $BaTiO_3$) in the second packed configuration has been also evaluated. Depending on the experimental conditions of applied voltage, residence time of reactants, feed ratios, or reactor configuration, different conversion yields are achieved ranging from 20 to 80% in the case of methane and 7−45% for the carbon dioxide. The direct decomposition of methanol reaches 60−100% under similar experimental conditions. Interestingly, the selectivity toward the production of hydrogen and carbon monoxide is kept almost constant under all the experimental conditions, and the formation of longer hydrocarbon chains or coke as a byproduct is not detected. The maximum efficiency yields are observed for the packed-bed reactor configuration containing alumina for both reaction processes (∼1 mol H_2 per kilowatt hour for dry reforming of methane and ∼4.5 mol H_2 per kilowatt hour for direct decomposition of methanol).

1. Introduction

The energy demand existing nowadays is mainly fulfilled by fossil sources such as coal, crude oil, or natural gas (the latter mainly composed of methane and carbon dioxide in different ratios, depending on the geographical location of the gas fields). Despite technological advances for more efficient detection of new fossil beds, their limited availability is contributing to the exponential increase in the prices of the raw material. In addition, their contribution to global warming and pollution can not be neglected. Therefore, there is a clear need for alternative clean fuels and greener synthesis routes. Hydrogen-based processes represent one of the most promising and widespread strategies currently under study. Other interesting approaches must be related to finding more economical and environmentally friendly uses for the current fossil feedstocks.

A very promising reaction is the dry reforming of methane (DRM), also known as carbon dioxide reforming of methane (eq 1; $\Delta H^0 = +247$ kJ mol^{-1}):[1−12]

$$CO_2(g) + CH_4(g) \rightarrow 2CO(g) + 2H_2(g) \qquad (1)$$

The use of two potential greenhouse effect sources, such as CO_2 and CH_4 to produce synthesis gas (syngas), a valuable precursor for the attaining of further chemicals, represents a highly attractive alternative.[1−8,13] In past years, several catalytic systems have been successfully developed for an optimal performance of the reaction. Ni-based systems have been denoted as the most suitable catalysts.[5,6,8,14] Nevertheless, some major drawbacks are still associated with this reaction, thereby preventing its application on an industrial scale: (i) the rapid deactivation of the catalysts due to the formation of coke, especially in Ni-based systems; (ii) the high temperature ranges required to achieve high conversion yields, thus meaning that additional burning of fossil fuel is required to achieve those high temperatures, thereby causing an additional output of CO_2 and making the energy conversion process less economically viable.

Another attractive process is related to the conversion of low-chain alcohols, such as methanol and ethanol, to obtain hydrogen or syngas.[5,7,15−27] They are considered excellent liquid H_2 sources with low toxicity and are attainable from the conversion of fossil fuels or natural sources such as biomass.[5,16,18] Their use, especially in the case of methanol, is mainly intended for hydrogen production for fuel cells and automotive applications, and different copper-based systems have been claimed among the most effective catalysts in the processes of direct decomposition (eq 2, $\Delta H^0 = +92$ kJ mol^{-1}), partial oxidation (eq 3, $\Delta H^0 = -192.2$ kJ mol^{-1}), or steam reforming of methanol (eq 4, $\Delta H^0 = +49.4$ kJ mol^{-1}).[19−21,27]

† Part of the special issue "Green Chemistry in Energy Production Symposium".

* To whom correspondence should be addressed. Address: Instituto de Ciencia de Materiales de Sevilla (ICMSE-CSIC), Avda Américo Vespucio, 43, Isla de la Cartuja (CICIC), 41092 Sevilla, Spain. Phone: (+34) 954489500. Fax: (+34) 954460665. E-mail: jhueso@icmse.csic.es. Web: www.sincaf-icmse.es.

‡ Instituto de Ciencia de Materiales de Sevilla.

§ Departamento de Química Inorgánica.

|| Departamento de Física Atómica, Molecular y Nuclear.

⊥ Present address: Department of Chemical Engineering, University of Texas at Austin, Austin, TX.

10.1021/jp100346q
Published on Web 02/25/2010

$$CH_3OH(g) \rightarrow CO(g) + 2H_2(g) \quad (2)$$

$$2CH_3OH(g) + O_2(g) \rightarrow 2CO_2(g) + 4H_2(g) \quad (3)$$

$$CH_3OH(g) + H_2O(g) \rightarrow CO_2(g) + 3H_2(g) \quad (4)$$

In the present work, we aimed at presenting the use of plasma technology as an alternative to carry out the dry reforming of methane (eq 1) and the direct decomposition of methanol (DDM) (eq 2) reactions working at ambient pressures and lower temperatures than required by conventional catalytic processes. Nonequilibrium plasmas are defined as highly excited gases composed of electrons, ions, atoms, and molecules with different energetic states.[28,29] Cold plasmas can be generated using different experimental setups, but dielectric-barrier-discharge (DBD) reactors have been shown to be very promising[28−31] for several reasons: (i) DBD configurations require low input powers to induce physical and chemical reactions within gases at relatively low temperatures (T < 200 °C); (ii) these plasma reactors can be operated at ambient pressure; (iii) the reactor design facilitates the scaling-up process to operate with higher volumes of gases; (iv) DBD devices have a well-established technology for ozone production; and (v) they show a high electron density and glow discharge extension.

All these characteristics have led to the systematic application of DBDs in different environmental processes,[28,31] especially in decontamination of pollutants and energy conversion processes.[1−4,9−11,29,32] Different groups have previously evaluated the dry reforming of methane with low-temperature plasmas.[1−4,9−11,29,32] The varieties of results are quite promising but at the same time very difficult to compare, especially in terms of conversion yields and selectivity of byproduct generated. The main reasons attributed to the difference in the results have to do with the great number of parameters influencing the generation of the discharge itself, as well as the differences in the initial concentrations and flow rates of the chemicals. Therefore, the systematic evaluation of these different parameters and the search for optimal reactors designs are still necessary to further develop the application of plasmas in the DRM reaction. On the contrary, the investigation and application of plasma technology for the conversion of alcohols is still scarce on the literature[23−27,33,34] and deserves further research.

Herein, we have explored different aspects related to the capability of two different DBD plasma setups in the carbon dioxide reforming of methane and the direct decomposition of methanol reactions to produce hydrogen and syngas as added-value products. A systematic study of the influence of different experimental parameters such as total flow rates, feed ratios, morphology (roughness) and composition of the electrodes has been carried out for the DRM reaction. In the case of methanol, a comparison between reactor configurations and the influence of different filling-gap dielectric materials (Al_2O_3 versus $BaTiO_3$) have been thoroughly studied. High conversions and efficiency yields are obtained for both reactions and reactor configurations under our experimental conditions, thereby showing a high and promising potential of plasma technology in C_1 chemistry processes.

2. Experimental Section

Two different plasma reactor configurations have been evaluated for the DRM and DDM reactions. The first setup consists of a DBD plasma reactor inspired by a previous design described elsewhere.[24] Herein, we present a modified version of the reactor to enable the study of the influence of roughness/porosity of the electrodes in the reaction efficiencies. The experimental arrangement used for the study is shown in Figure 1 and consists of the following parts: (1) A stainless steel cylinder with controlled roughness in the zone of the plasma discharge with holes for the gas inlet just at the beginning of the discharge zone. We investigated three electrodes with different induced morphologies. The first one was sandblasted, thereby creating 1 μm depth irregularities; another cylinder consisted of porous stainless steel that introduced the gases inside the zone of the plasma discharge; and the third type of cylinder contained 3 mm holes around the discharge area (Figure 1). (2) Inlet and circulation of gases. (3) A quartz tube acting as a dielectric barrier. This quartz tube has an outer diameter of 25 mm and a wall thickness of 2 mm. (4) A metal electrode made of stainless steel with an aluminum belt externally covering the dielectric tube. The area covered by this external electrode defines the zone where the plasma is produced. (5) An external furnace to maintain the reactor at temperatures higher than 110 °C to avoid condensation of water. A critical parameter of the production of plasma inside the reactor is the distance between the rough surface of the inner stainless steel cylinder and the dielectric tube. This distance lies between 1 and 3 mm. Total volume of the empty space in the reactor was between 7 and 15 cm^3.

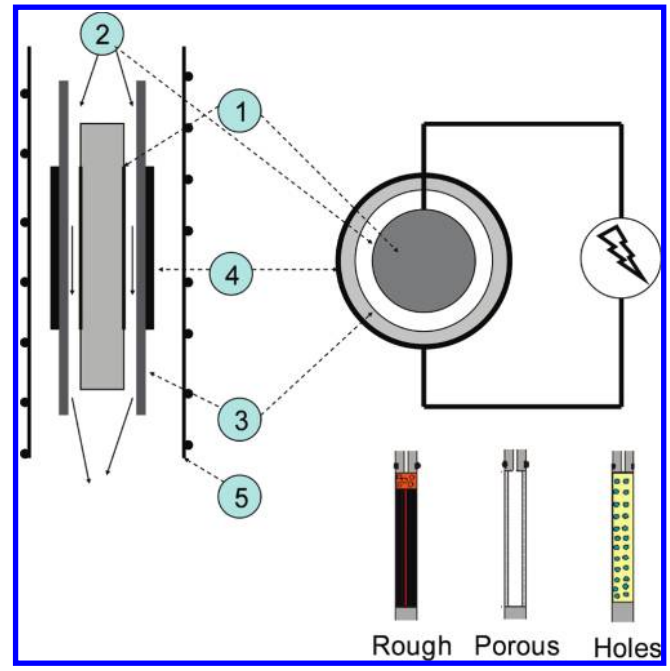

Figure 1. Schematic representation of the first DBD plasma configuration. The insets represent the different electrodes' roughness and morphologies under study (see text). The different parts of the reactor and their corresponding assignation with numbers are fully described within the text.

The second DBD configuration under study has been previously defined as a packed-bed reactor.[32] As a result, a more robust and industrially scalable reactor was developed. In this setup, the external electrode is entirely made of stainless steel. In addition, the gap between the electrodes is filled with different dielectric materials. The experimental setup is schematically described in the Figure 2: (1) a stainless steel cylinder without controlled roughness and 30 mm in diameter; (2) the inner electrode covered with an alumina cylinder (3 mm thickness) or, alternatively, filled with ferroelectric pellets of $BaTiO_3$ (200 gr purchased from Alfa Aesar) on the order of 2−3 mm acting

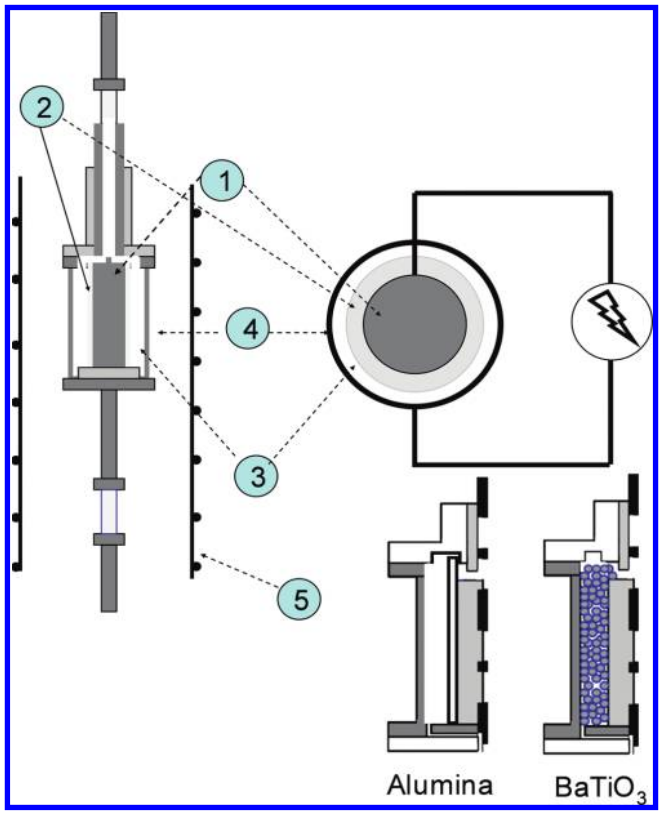

Figure 2. Schematic representation of the second packed-bed DBD plasma configuration. The insets represent the midsection sketch of the reactors packed with an alumina cylinder and ferroelectric $BaTiO_3$ beads, respectively. The different parts of the reactor and their corresponding assignation with numbers are fully described within the text.

as dielectrics; (3) inlet and circulation of gases in downstream mode; (4) a metal electrode made of stainless steel with 38 mm of internal diameter (the length of this external electrode defines the zone where the plasma is produced); and (5) an external furnace to maintain the reactor at temperatures higher than 110 °C to avoid condensation of water. The whole setup was protected with a Teflon cylinder.

An AC power supply whose voltage can be varied between 1 and 30 kV and its frequency between 750 and 6 kHz has been used to ignite the plasma. The power source has a bipolar configuration with two electric transformers in the output. Each transformer is connected to each electrode in counter-phase, providing a maximum voltage of 15 kV. The electrical characterization of the source was made with a digital oscilloscope (Tektronix TDS3034B). The typical voltage and current waveforms obtained for both reactor configurations are depicted in Figure 3. The presence of spikes or sharp peaks in the current curves is characteristic of microarc formation.[12,24,35] These filaments are generated when positive or negative voltages induce a local electric field that causes the electric breakdown of the gas throughout the surface of the electrodes.[12,24,35] Hence, the present architecture of the bipolar power source gives remarkable characteristics to the discharge so that filaments occur not only at the rising edge but also at the falling edge of the applied voltage (Figure 3). Different mixtures of carbon dioxide and methane or methanol were adjusted by mass flow controllers (Bronkhorst). The gas line was heated at around 110 °C to avoid any condensation of water. The reaction products were analyzed with a mass spectrometer (Sensorlab) placed downstream of the reactor. This mass spectrometer was carefully calibrated with mixtures of the pure gases to quantify the

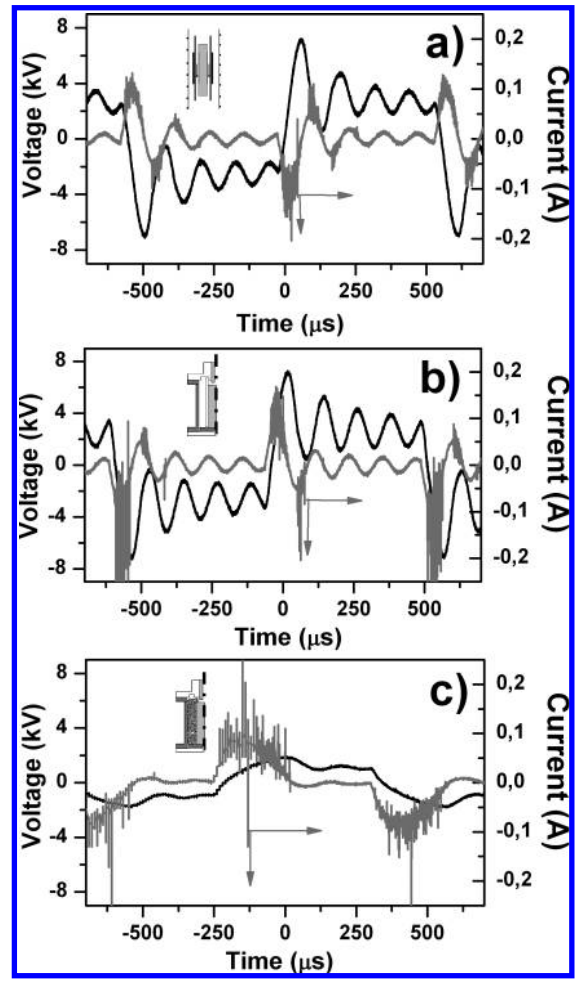

Figure 3. Typical voltage (black lines) and current (gray lines) waveforms for the different reactor configurations. The applied frequency was 900 Hz. The spectra correspond to the direct decomposition of methanol (total flow = 5 sccm).

reaction efficiency for all experimental conditions. A maximum uncertainty of 10% was estimated for our experimental conditions.

The determination of the power density, an important factor to associate with the efficiency and the economical viability of the process, is not yet completely understood for these types of systems. Plasmas in DBDs are normally characterized by a large number of microdischarges per unit of electrode area and per cycle, since the lifetimes of these microdischarges are in the range of the nanoseconds.[29] A typical value is about 10^6 microdischarges cm^{-2} s^{-1}.[36] For many purposes, it is sufficient to describe the discharge by overall quantities: the applied frequency, f; the maximum applied voltage, V_{peak}; and finally, the minimum external voltage at which microdischarges are observed in the discharge gap, V_{ig}. The interesting feature of the DBD power formula first proposed by Manley[37] is that only the peak value of the applied voltage is necessary, and not its form.

$$P = 4V_{ig}C_{die}f\left[V_{peak} - \left(\frac{C_{die} - C_{gas}}{C_{die}}\right)V_{ig}\right] \qquad (5)$$

Expression 5 correlates the total power, P, and the operating frequency, f; the peak voltage V_{peak}; and the capacitances of the dielectric(s) C_{die} and the discharge gap, C_{gas}, quantities that characterize the electrode configuration. The discharge voltage

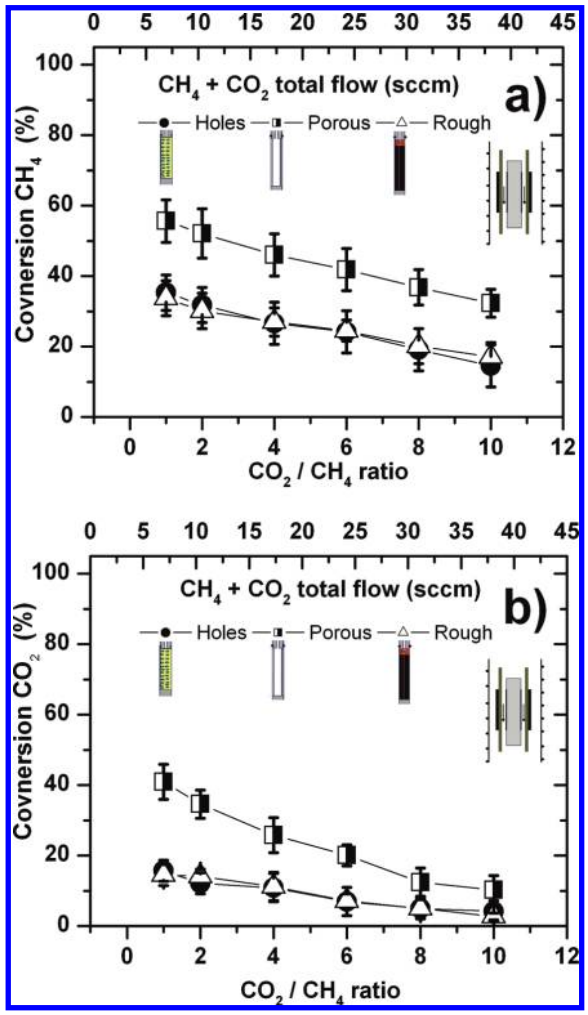

Figure 4. Evaluation of the conversion of (a) CH_4 and (b) CO_2 in the dry reforming of methane under different feed ratios, residence times, and electrode roughnesses. The frequency applied was 900 Hz.

depends on the nature of the gas mixture, the gas density, and the width of the discharge gap. For this characterization, we take into account the region of cycle where there is discharge between the two electrodes. The remaining cycle is associated with an electrode configuration where no plasma is generated.[30] Depending on the peak voltage, the microdischarge activity is limited to a certain fraction of the cycle and occurs at twice the driving frequency. The reaction efficiencies were calculated in terms of the power density (i.e., applied voltages and frequencies) and the total flows and conversion of reactants (i.e., methane or methanol) expressed in moles of H_2 converted per kilowatt and per hour.[9]

3. Results

3.1. Influence of Total Flow Rate. The total feed flow rate is directly associated with the residence time of the reactants within the reactor. Figure 4a shows the influence of increasing the total flow of CH_4-CO_2 in the final conversion yields of methane. A similar trend is observed for all the DBD configurations, regardless of the roughness degree of the electrodes (first DBD configuration). Increasing the total flow rate from 7 to 40 sccm causes an overall 20% decrease in the CH_4 conversion yields (from 60 to 40% in the porous-electrode configuration and from 40 to 20% for the blasted and hole−electrode ones). Analogously, CO_2 conversion yields are also reduced with increasing feed rates, as depicted in Figure 4b. The selectivity

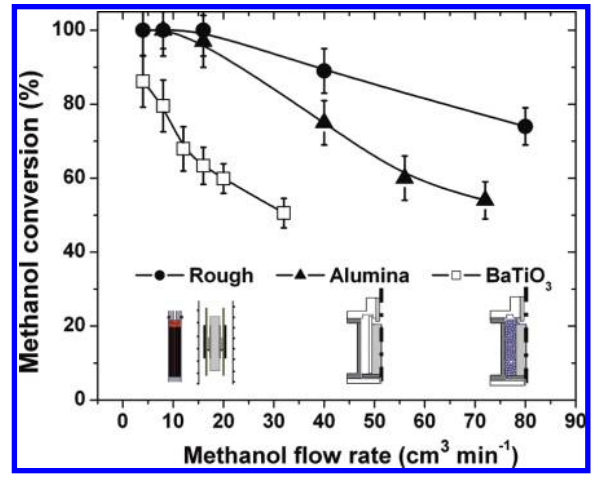

Figure 5. Evaluation of the influence of the total flow rate on the conversion of methanol for different reactor configurations. The frequency applied was 900 Hz.

of the final products is not affected, and CO, H_2, and some traces of water are identified for all the experimental conditions.

In the decomposition of methanol reaction, a similar influence on the DRM reaction is observed, and increasing the flow rates decreases the methanol conversion. Figure 5 shows the different conversion levels and total flows evaluated. The use of the first DBD configuration with the sandblasted electrode yields the maximum conversion levels (100−78%) for the widest range of flow rates (3.5−80 cm^3 min^{-1}). A frequency of 900 Hz and an applied voltage of 30 kV are the constant plasma parameters for this experiment. Similar conditions were applied in the packed-bed reactor (second DBD configuration) containing the alumina cylinder as the dielectric material. In this case, the conversion levels of methanol are reduced by 45% with increasing feed rates (cf. Figure 5). Finally, the ferroelectric packed-bed configuration with $BaTiO_3$ beads could be evaluated only for a maximum flow rate of 30 cm^3 min^{-1} (the maximum flow to keep a stable discharge), showing the lowest conversion levels and the same detrimental effect of reducing the residence time of the reactants within the reactor bed. In this latter case, methanol conversions from 88 to 50% are detected upon increasing the methanol flow rate. Interestingly, the total applied voltage is kept within 2−3 kV in comparison with the higher values applied for the rest of the configurations (i.e., 25−30 kV). CO and H_2 were the only byproducts monitored throughout all the experiments and for all the DBD configurations. No signs of coke deposits or longer hydrocarbon formation were detected.

3.2. Influence of CO_2/CH_4 Ratios. Figure 4 shows the evaluation of different CO_2/CH_4 mixing ratios in the methane (Figure 4a) and carbon monoxide conversion yields (Figure 4b). A working frequency of 900 Hz and a consuming voltage of 30 kV were applied for the different mixtures and DBD reactor configurations. The input of CH_4 was kept constant at 3.5 sccm while the CO_2 flow rates were increased up to 37.5 sccm. Increasing the proportion of CO_2 in the feed does not affect the attainment of CO and H_2 as main products, but the decreasing conversion trend is observed equally for both CH_4 and CO_2 at the same time and for the all the reactor configurations. A major influence of the change of the residence time (space velocity) due to the increment of total feed flows must be attributed instead as discussed in the previous section. Nevertheless, the appearance of some minority byproduct due to the variation of compositions cannot be discarded. For instance, if CO_2 is not present in the mixture (results not shown), some carbonaceous species start to deposit on the reactor. Conversely, when the

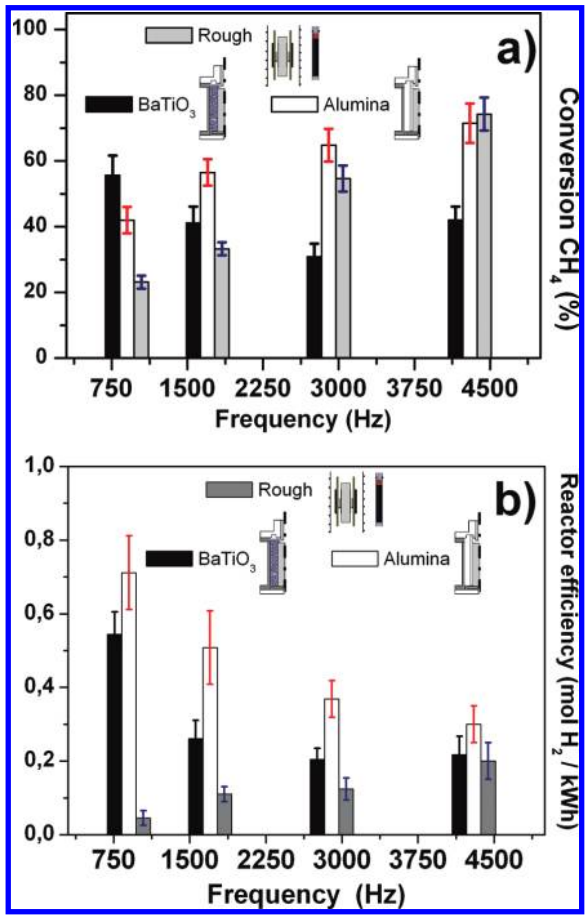

Figure 6. Evaluation of the influence of the applied frequency on (a) the conversion of CH_4 and (b) the reaction efficiency expressed in moles of H_2 per kilowatt hour. The total flow of CH_4 and CO_2 was fixed at 6 and 12 sccm, respectively.

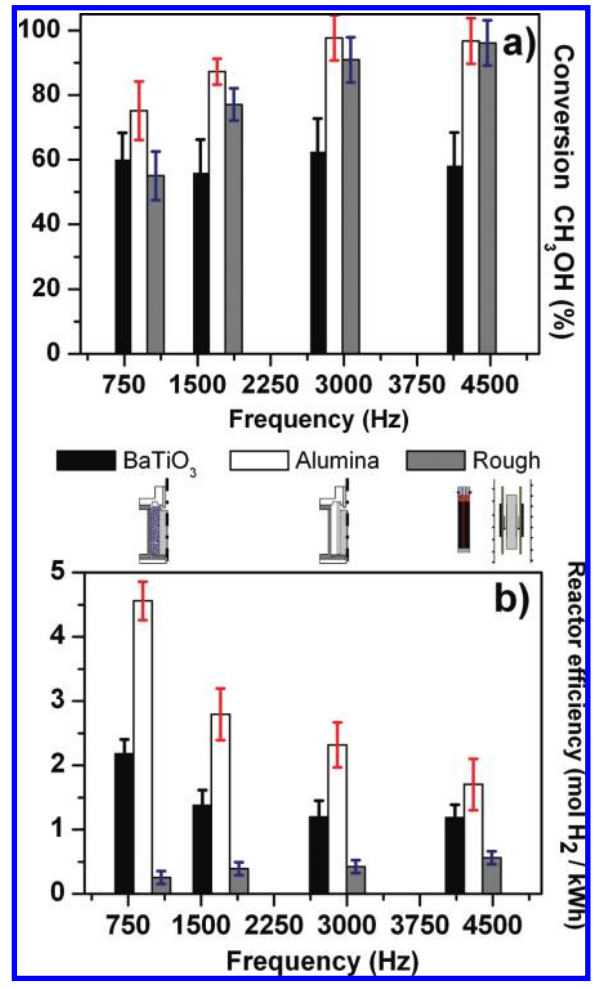

Figure 7. Evaluation of the influence of the applied frequency on (a) the conversion of CH_3OH and (b) the reaction efficiency expressed in moles of H_2 per kilowatt hour. The total flow of CH_3OH was fixed at 20 μL for the rough configuration and at 40 μL for the packed-bed reactor with alumina or $BaTiO_3$.

CO_2/CH_4 ratio exceeds a value of 6 (Figure 4), some traces of water are detected, thus meaning that the reverse WGS reaction is partially taking place (eq 6; $\Delta H^0 = +41.2$ kJ mol^{-1})9:

$$CO_2(g) + H_2(g) \rightarrow CO(g) + H_2O(g) \qquad (6)$$

We conclude that the overall variations in the selectivity to H_2 and CO as well as the effect of increasing the amount of CO_2 under our experimental conditions can be considered negligible.

3.3. Influence of Discharge Power. After fixing CH_4 and CO_2 flow rates to 6 and 12 sccm, respectively, a systematic study of the effect of increasing the frequency (thus increasing the power density according to the Manley equation, see eq 5) in the conversion yields was carried out. Three different reactor configurations were studied and compared: (i) the DBD configuration with the rough electrode, (ii) a packed-bed configuration with Al_2O_3, and (iii) a packed-bed reactor with $BaTiO_3$. In the case of the methanol decomposition reaction, similar experimental conditions were chosen for a total flow of 5 μL min^{-1}.

Figure 6a shows how the increase in the frequency from 750 to 4500 Hz supposes a systematic increase in methane conversion for the DBD rough configuration and the packed-alumina reactor. However, the influence of power is shown more pronounced in the DBD rough configuration with an increasing methane conversion yield from 20% at the lowest frequency of 750 Hz up to 75% for 4500 Hz. In the alumina reactor, methane conversion rises with the input power to similar levels, but it is initially better (40% minimum conversion at 750 Hz). Interestingly, the second packed-bed reactor containing $BaTiO_3$ shows an opposite trend and exhibits maximum conversion yields at 750 Hz (almost 60%). Increasing the frequency has a detrimental effect and lowers the total conversion of methane to a minimum of 30% at 3000 Hz, slightly improved to 40% for the maximum frequency evaluated (Figure 6a). CO_2 yields followed a conversion trend similar to that described for methane but always showing lower levels between 5 and 40%. Additionally, it must be pointed out that the selectivity to CO and H_2 is not affected by the increasing frequency.

As shown in Figure 7a, the methanol conversion yields are higher for all the frequencies applied and all the reactor configurations in comparison with the DRM reaction (Figure 6a). The lower conversions are observed again for the packed-bed reactor with the $BaTiO_3$ perovskite. The yields keep constant around 60% regardless of the applied frequencies. Conversely, the increase in the discharge power enhances the methanol conversion yield for the two other reactor configurations. The packed-bed alumina reactor reaches 92% conversion at 4500 Hz. In the DBD rough reactor, a similar yield is obtained at high frequencies, but the conversion levels are below 60% for the lower frequency values (Figure 7a). As previously observed for the DRM experiments, the selectivity to syngas (CO and H_2) is not altered by the increase in the discharge power in any of the reactor configurations.

3.4. Reaction Efficiencies. Another important parameter to consider is the efficiency of the process and the energetic balance for the conversion of reactants to obtain valuable products. In our case, we have referred the reactor efficiency to the power necessary to convert methane or methanol into hydrogen (expressed in terms of moles of H_2 per kilowatt hour). The determination of the energy input is done through the Manley equation[29,30,37] and the $I-V$ curves (Figure 3) corresponding to each reactor configuration. Figure 6b shows how the reactor efficiencies in the dry reforming of methane are really dependent on the type of plasma reactor and the input frequency. Both packed-bed configurations follow a similar trend and show lower efficiencies with increasing input powers. The DBD rough configuration shows the opposite effect and slightly raises the reaction efficiency from 0.05 to 0.2 mol H_2/kWh when increasing the applied frequency from 750 to 4500 Hz. Nevertheless, these values are far from those obtained for the packed-bed reactors, especially at the lower applied frequencies (∼0.5 mol H_2/kWh for the reactor containing $BaTiO_3$ and 0.7 mol H_2/kWh for the alumina reactor).

In the case of the direct methanol decomposition, the reaction efficiency trends observed for each reactor configuration are quite similar to the DRM experiments (see Figure 7b). However, the efficiency values are much higher than those obtained for the methane reforming reaction. Again, it is shown how the DBD rough configuration yields the less energetic favorable values with 0.5−0.7 mol H_2/kWh. The packed bed with $BaTiO_3$ reaches an energy efficiency of ∼2 mol H_2/kWh, which slightly diminishes to 1.5 when the frequency rises. Similarly, the other packed-bed reactor containing alumina reaches 4.5 mol H_2/kWh values of energetic efficiency reduced to 1.8 mol H_2/kWh at the maximum input power (Figure 7b). Even under the least favorable conditions, the conversion of methanol into hydrogen is at least 3 times more efficient than the corresponding conversion of methane under the same reactor and plasma conditions (Figure 6 b and 7b).

4. Discussion

4.1. Dry Reforming of Methane (DRM). One key parameter under study in the present work has been the systematic evaluation of different reactor configurations and their contribution to the overall reaction efficiencies and conversion yields for the carbon dioxide reforming of methane. Furthermore, specific attention has been paid to a novel aspect such as the influence of the surface morphology of the inner electrodes. Previous studies presented by Choi et al.[38] suggested better plasma homogeneity after coating the electrodes with ZnO/Al_2O_3 rough films. Preliminary results in our group also envisioned that providing some roughness to the initially flat inner electrode was an important parameter to take into account.[24] Herein, after comparing three electrodes with different surface textures (see the Experimental Section), we have been able to confirm the better performance of the reactor in comparison with the smoother electrode version working under identical experimental conditions.[24] Moreover, we observed that the best conversion yields were achieved with the most porous electrode (cf. Figure 4). Up to 60% of methane conversion was obtained, almost 20% higher than the electrode with 3 mm holes or the sandblasted one (Figure 4a). A possible explanation for the better reaction yields observed in the porous DBD reactor might be attributed to the better immobilization of gas molecules within the intraporous network of the electrode, thereby creating additional active sites for the interaction with short-lived excited intermediates. This hypothesis has already been proposed by other authors for the remediation of volatile organic compounds (VOCs) in the presence of plasmas and porous alumina or silica.[39−43] Nevertheless, a scalable version of this porous DBD prototype would not be economically viable due to the prohibitive cost of fabrication of the electrode with that specific morphology. In addition, the high applied voltages (close to 30 kV) and the relatively low reaction efficiencies obtained (<0.2 mol H_2/kWh) made the DBD configuration less energetically competitive than other systems available in the literature.[1,9] These economical burdens were the main motivation to explore a different DBD reactor approach based on a packed-bed configuration.[32]

Built on low cost and easy-to-assembly components, a more robust, manageable, and industrial scalable reactor could be developed (cf. Figure 2). Figure 6 accounts for the different conversion yields of methane and reaction efficiencies obtained in the DRM reaction when comparing one of the first DBD configurations (rough electrode) with the packed-bed versions filled with a porous alumina cylinder or $BaTiO_3$ beads, respectively (see insets in Figure 2). Higher conversion yields were obtained for the new configurations, especially at low frequency values of 750 Hz (cf. Figure 6a). Although the conversion levels for the rough first DBD configuration were comparable or even better with increasing power density, the main differences were definitely observed in terms of reaction efficiencies (Figure 6b). Values of 0.5 mol H_2/kWh (or ∼0.15 mmol H_2/kJ) and 0.7 mol H_2/kWh (or ∼0.20 mmol H_2/kJ) were achieved for the $BaTiO_3$ and the alumina-packed reactors, respectively. This meant an order of magnitude higher than the rough DBD reactor under the same experimental conditions and similar efficiency levels compared with other systems.[1,9] Likewise, the applied voltage in the $BaTiO_3$ reactor was within 2−3 kV, whereas the other configurations oscillated around 30 kV, yielding the most energetic competitive configuration. Thus, the better conversion and efficiency results obtained with the alumina reactor should be attributed to certain additional catalytic abilities of the dielectric material itself, as has been previously claimed for other plasma-catalytic systems.[39−43]

Another important aspect systematically observed in the DRM reaction under our experimental conditions was that CO_2 rendered lower conversion percentages than methane. In all cases, the values were ∼20% below the conversion levels achieved for the hydrocarbon coreactant. This phenomenon has been similarly described by numerous authors.[1−4,9−13,44−51] Bo et al.[44] explained this difference on the basis of the higher dissociation energy of CO_2 (bond dissociation energy = 5.52 eV) in comparison with that of CH_4 (bond dissociation energy = 4.55 eV). Similarly, Wang et al.[13] determined that the ionization energy required for CO_2 was higher than for CH_4 (13.8 and 12.9 eV, respectively); thus, the former was more stable and less reactive within the plasma discharge. Finally, other authors have claimed the existence of a competitive reaction to form CO_2: ($OH^* + CO^* \rightarrow CO_2 + H^*$).[44,52] Anyway, the methane conversion yields showed no significant dependence on increasing the feed percentage of CO_2 (Figure 4a). Furthermore, even under experimental conditions when CH_4 was predominant, no sign of carbonaceous deposits or longer hydrocarbon chain formations was detected, in comparison with other plasma configurations.[9−13,46,51−54] The selectivity toward $CO + H_2$ formation was kept almost constant, and only small traces of water formation, probably due to reverse-WGS (eq 6), were identified with increasing CO_2 contents. This same trend was also shown by Song et al. in their noncatalytic plasma reactor.[46,49] Methane dissociates under the influence of the

reactive plasma conditions, yielding carbonaceous particles, higher hydrocarbons, or both.[11,46,50,52−56] In our opinion, the main factors preventing the formation of these nondesired byproducts have to do with (i) the role of CO_2 to scavenge any coke formation and produce CO as the only byproduct (differs from O_2 as oxidant agent, since does not generate gas phase radical reactions and oxygenate intermediate species so easily),[9,46] (ii) the absence of a catalyst within the discharge to increase the selectivity toward C_2 species,[2,3,10,46,51] and (iii) the use of a bipolar configuration source that duplicates the formation of filament discharges at both the falling and rising edges of the applied voltage.[24,48,49]

4.2. Direct Decomposition of Methanol (DDM). As previously pointed out in the Introduction, alcohols in general and methanol in particular represent one of the most promising alternatives to fossil fuels as cleaner energy sources.[18] Hydrogen can be easily stored and handled in the form of liquid alcohol, thereby avoiding the use of high-pressure conditions, risks of leakage and explosions, and exhaustive storage and safety protocols.[5,16,18,20,57] In addition, part of these alcohols can be obtained from natural resources (i.e., biomass).[5,16,18,57] Although great efforts are being made to develop efficient catalytic processes for the reforming or direct decomposition of alcohols,[7,8,14,19−23,58] the application of plasma discharges for this purpose is still surprisingly scarce in the literature.[23−27,33,34]

One of the most remarkable results obtained within the frame of the present work has consisted of the attainment of high conversion yields of methanol into hydrogen and carbon monoxide (Figures 5 and 7) without the formation of other byproducts such as carbon deposits or higher hydrocarbons. Preliminary results in our group showed that the reforming of ethanol by a microwave-assisted surfatron launcher yielded carbon deposits on the walls and acetylene (C_2H_2) in the absence of a second oxidant agent such as water.[23] Nevertheless, local heating effects generated by the microwave irradiation could be inducing the formation of these carbon deposits.

According to this, our first reforming experiments with alcohols using a DBD configuration were made with the partial addition of water to prevent the formation of coke.[24] To our surprise, all the experiments made subsequently with the configurations described in this work could be initially carried out in the absence of water without the formation of carbonaceous particles. Therefore, direct decomposition of methanol (see eq 2), a reaction that is thermodynamically unfavorable, was instead plausible under the nonequilibrium energetic conditions of plasmas. Initially, we attributed this fact to the rough morphology of the new inner electrode in the first DBD configuration. However, after some preliminary attempts reforming methane alone (results not shown) in which carbon started to deposit, we finally came up with the conclusion that the formation of hydroxyl radicals (OH*) from the direct decomposition of methanol was preventing the formation of carbonaceous species.[23,25,59−61]

In terms of a comparison of methanol conversion yields for the different plasma DBD configurations under study, better results were obtained with the first DBD device and the rough electrode (Figure 5). In addition, the detrimental effect of reducing the residence times (i.e., increasing flow rates) was less pronounced for this configuration and enabled up to 80% conversion levels working with an applied frequency of 900 Hz and feed rates of 80 sccm. The packed-bed reactor with alumina rendered quite similar results, but the maximum conversion capacity was kept below 60% for the higher flow rates. Both configurations required voltage values (25−30 kV) identical to those previously described for the DRM reaction.

Conversely, the second packed-bed reactor with $BaTiO_3$ required only 2 kV and reached 50% under the least favorable conditions (i.e., minimum residence time). Hence, when the systematic influence of increasing the applied frequency (the power density) was studied, this latter reactor gave the most stable and reproducible results and maintained similar methanol conversion percentages (around 60%) (Figure 7a) and energy efficiencies over 1.5 mol H_2/kWh (Figure 7b) (better than any result with the DRM reaction; see the previous section). The rough DBD and the packed-bed with alumina reactors exhibited a noticeable increase in the conversion levels with increasing power discharge, almost reaching total conversion levels (Figure 7a). Nevertheless, in terms of efficiency, the first DBD configuration barely reached 0.5 mol H_2/kWh, whereas the latter showed the best results for every applied frequency. The high applied voltage values made the reactor less efficient with the increasing power density (Figure 7b), but even under those experimental conditions, efficiency levels oscillated between 4.5 and 1.8 mol H_2 per kWh. As previously pointed out, the high specific surface area of alumina can be providing additional reaction sites and behaving as a catalyst within the reactor discharge.[39,40]

The overall higher conversion yields and reaction efficiencies found in comparison with the dry reforming of methane reaction must be associated with the lower bond dissociation energy for methanol[25] (4.16 eV) and the oxidizing contribution from the hydroxyl radicals released under the influence of the plasma discharge. The presence of OH* intermediates has been proved to be beneficial for the reforming of hydrocarbons and carbonaceous species.[23,24,27,60] Nevertheless, in our opinion, future efforts in this relatively unexplored field should be focused on the development of a versatile reactor that permits a better control of the stoichiometry of the final byproduct. In this regard, recent results by Rico et al.[27] have demonstrated that the combination of the $BaTiO_3$ packed reactor with certain amounts of Cu−Mn catalysts can increase the selectivity of the final product CO into CO_2. This result can foster the extrapolation to the fuel cells and the proton exchange membrane fields where carbon monoxide would act as a poison for the Pt electrode.

5. Conclusions

Different DBD plasma configurations were investigated for the dry reforming of methane and the direct decomposition of methanol reactions. In the first reactor, the roughness of the inner electrodes was demonstrated to play an important role on the conversion and efficiency levels of methane. However, the best results were obtained for the packed-bed configuration based on a more robust, manageable and scalable design and more efficiency, especially at lower frequency inputs. On the other hand, the decomposition of methanol yielded higher conversion percentages and better energy efficiencies for the production of hydrogen than the reforming of methane and constituted a novel and promising reaction in which the synergetic combination of plasmas and catalysts might play a decisive role in the final application for hydrogen production and fuel cells. The use of a bipolar source also facilitated an elevated selectivity of the byproduct toward CO and H_2 and the absence of carbon deposits or higher hydrocarbons.

Acknowledgment. The authors thank the Spanish Ministry of Education and Science for financial support. Part of this work has been carried out within a collaboration project with the company Hynergreen (Seville, Spain).

References and Notes

(1) Li, D. H.; Li, X.; Bai, M. G.; Tao, X. M.; Shang, S. Y.; Dai, X. Y.; Yin, Y. X. *Int. J. Hydrogen Energy* **2009**, *34*, 308.
(2) Kraus, M.; Egli, W.; Haffner, K.; Eliasson, B.; Kogelschatz, U.; Wokaun, A. *Phys. Chem. Chem. Phys.* **2002**, *4*, 668.
(3) Kraus, M.; Eliasson, B.; Kogelschatz, U.; Wokaun, A. *Phys. Chem. Chem. Phys.* **2001**, *3*, 294.
(4) Zhang, Y. P.; Li, Y.; Wang, Y.; Liu, C. J.; Eliasson, B. *Fuel Process. Technol.* **2003**, *83*, 101.
(5) Navarro, R. M.; Peña, M. A.; Fierro, J. L. G. *Chem. Rev.* **2007**, *107*, 3952.
(6) Martinez, R.; Romero, E.; Guimon, C.; Bilbao, R. *Appl. Catal., A* **2004**, *274*, 139.
(7) Sánchez-Sánchez, M. C.; Navarro, R. M.; Fierro, J. L. G. *Catal. Today* **2007**, *129*, 336.
(8) Steinhauer, B.; Kasireddy, M. R.; Radnik, J.; Martin, A. *Appl. Catal., A* **2009**, *366*, 333.
(9) Brock, S. L.; Shimojo, T.; Suib, S. L.; Hayashi, Y.; Matsumoto, H. *Res. Chem. Intermed.* **2002**, *28*, 13.
(10) Eliasson, B.; Liu, C. J.; Kogelschatz, U. *Ind. Eng. Chem. Res.* **2000**, *39*, 1221.
(11) Li, Y.; Xu, G. H.; Liu, C. J.; Eliasson, B.; Xue, B. Z. *Energy Fuels* **2001**, *15*, 299.
(12) Li, M. W.; Xu, G. H.; Tian, Y. L.; Chen, L.; Fu, H. F. *J. Phys. Chem. A* **2004**, *108*, 1687.
(13) Wang, Q.; Yan, B. H.; Jin, Y.; Cheng, Y. *Plasma Chem. Plasma Process.* **2009**, *29*, 217.
(14) Pholjaroen, B.; Laosiripojana, N.; Praserthdam, P.; Assabumrungrat, S. *J. Ind. Eng. Chem.* **2009**, *15*, 488.
(15) Huber, G. W.; Iborra, S.; Corma, A. *Chem. Rev.* **2006**, *106*, 4044.
(16) Corma, A.; Iborra, S.; Velty, A. *Chem. Rev.* **2007**, *107*, 2411.
(17) Llorca, J.; de la Piscina, P. R.; Sales, J.; Homs, N. *Chem. Commun.* **2001**, 641.
(18) Olah, G. A. *Angew. Chem., Int. Ed.* **2005**, *44*, 2636.
(19) Papavasiliou, J.; Avgouropoulos, G.; Ioannides, T. *Catal. Commun.* **2005**, *6*, 497.
(20) Papavasiliou, J.; Avgouropoulos, G.; Ioannides, T. *J. Catal.* **2007**, *251*, 7.
(21) Papavasillou, J.; Avgouropoulos, G.; Ioannides, T. *Catal. Commun.* **2004**, *5*, 231.
(22) Sato, T.; Kambe, M.; Nishiyama, H. *JSME Int. J. Ser. B, Fluids Therm. Eng.* **2005**, *48*, 432.
(23) Yanguas-Gil, A.; Hueso, J. L.; Cotrino, J.; Caballero, A.; González-Elipe, A. R. *Appl. Phys. Lett.* **2004**, *85*, 4004.
(24) Sarmiento, B.; Brey, J. J.; Viera, I. G.; González-Elipe, A. R.; Cotrino, J.; Rico, V. J. *J. Power Sources* **2007**, *169*, 140.
(25) Kabashima, H.; Einaga, H.; Futamura, S. *IEEE Trans. Ind. Appl.* **2003**, *39*, 340.
(26) Jiménez, M.; Yubero, C.; Calzada, M. D. *J. Phys. D: Appl. Phys.* **2008**, *41*, 175201.
(27) Rico, V. J.; Hueso, J. L.; Cotrino, J.; Gallardo, V.; Sarmiento, B.; Brey, J. J.; González-Elipe, A. R. *Chem. Commun.* **2009**, 6192.
(28) Penetrante, B. M.; Schultheis, S. E. *Non-Thermal Plasma Techniques for Pollution Control. Parts A and B*; Springer: Berlin, 1993.
(29) Kogelschatz, U. *Plasma Chem. Plasma Process.* **2003**, *23*, 1.
(30) Kogelschatz, U. *Advanced Ozone Generation in Process Technologies for Water Treatment*; Stucki, S., Ed.; Plenum Press: New York & London, **1988**, 87.
(31) Penetrante, B. M.; Brusasco, R. M.; Merritt, B. T.; Vogtlin, G. E. *Pure Appl. Chem.* **1999**, *71*, 1829.
(32) Kim, H. H. *Plasma Process. Polym.* **2004**, *1*, 91.
(33) Futamura, S.; Kabashima, H. *IEEE Trans. Ind. Appl.* **2004**, *40*, 1459.
(34) Tanabe, S.; Matsuguma, H.; Okitsu, K.; Matsumoto, H. *Chem. Lett.* **2000**, *10*, 1116.
(35) Eliasson, B.; Kogelschatz, U. *IEEE Trans. Plasma Sci.* **1991**, *19*, 1063.
(36) Coogan, J. J.; Sappey, A. D. *IEEE Trans. Plasma Sci.* **1996**, *24*, 91.
(37) Manley, T. C. *Trans. Electrochem. Soc.* **1943**, *84*, 83.
(38) Choi, J. H.; Il Lee, T.; Han, I.; Oh, B. Y.; Jeong, M. C.; Myoung, J. M.; Baik, H. K.; Song, K. M.; Lim, Y. S. *Appl. Phys. Lett.* **2006**, 89.
(39) Heintze, M.; Pietruszka, B. *Catal. Today* **2004**, *89*, 21.
(40) Holzer, F.; Roland, U.; Kopinke, F. D. *Appl. Catal., B* **2002**, *38*, 163.
(41) Chen, H. L.; Lee, H. M.; Chen, S. H.; Chang, M. B.; Yu, S. J.; Li, S. N. *Environ. Sci. Technol.* **2009**, *43*, 2216.
(42) Hueso, J. L.; Cotrino, J.; Caballero, A.; Espinós, J. P.; González-Elipe, A. R. *J. Catal.* **2007**, *247*, 288.
(43) Hueso, J. L.; Caballero, A.; Cotrino, J.; González-Elipe, A. R. *Catal. Commun.* **2007**, *8*, 1739.
(44) Bo, Z.; Yan, J. H.; Li, X. D.; Chi, Y.; Cen, K. F. *Int. J. Hydrogen Energy* **2008**, *33*, 5545.
(45) Huang, A. M.; Xia, G. G.; Wang, J. Y.; Suib, S. L.; Hayashi, Y.; Matsumoto, H. *J. Catal.* **2000**, *189*, 349.
(46) Istadi, Amin N. A. S. *Fuel* **2006**, *85*, 577.
(47) Jiang, T.; Li, Y.; Liu, C. J.; Xu, G. H.; Eliasson, B.; Xue, B. Z. *Catal. Today* **2002**, *72*, 229.
(48) Lee, H.; Lee, C. H.; Choi, J. W.; Song, H. K. *Energy Fuels* **2007**, *21*, 23.
(49) Song, H. K.; Lee, H.; Choi, J. W.; Na, B. K. *Plasma Chem. Plasma Process.* **2004**, *24*, 57.
(50) Zhang, K.; Eliasson, B.; Kogelschatz, U. *Ind. Eng. Chem. Res.* **2002**, *41*, 1462.
(51) Zhang, K.; Kogelschatz, U.; Eliasson, B. *Energy Fuels* **2001**, *15*, 395.
(52) Yao, S. L.; Okumoto, M.; Nakayama, A.; Suzuki, E. *Energy Fuels* **2001**, *15*, 1295.
(53) Li, X. S.; Zhu, A. M.; Wang, K. J.; Yong, X.; Song, Z. M. *Catal. Today* **2004**, *98*, 617.
(54) Ghorbanzadeh, A. M.; Norouzi, S.; Mohammadi, T. *J. Phys. D: Appl. Phys.* **2005**, *38*, 3804.
(55) Heintze, M.; Magureanu, M.; Kettlitz, M. *J. Appl. Phys.* **2002**, *92*, 7022.
(56) Hueso, J. L.; González-Elipe, A. R.; Cotrino, J.; Caballero, A. *J. Phys. Chem. A* **2005**, *109*, 4930.
(57) Corma, A.; Huber, G. W.; Sauvanaud, L.; O'Connor, P. *J. Catal.* **2007**, *247*, 307.
(58) Yao, S.; Zhang, X.; Lu, B. *AICHE J.* **2005**, *51*, 1558.
(59) Hueso, J. L.; Rico, V. J.; Cotrino, J.; Jimenez-Mateos, J. M.; Gonzalez-Elipe, A. R. *Environ. Sci. Technol.* **2009**, *43*, 2557.
(60) Hueso, J. L.; Espinós, J. P.; Caballero, A.; Cotrino, J.; González-Elipe, A. R. *Carbon* **2007**, *45*, 89.
(61) Chen, X.; Marquez, M.; Rozak, J.; Marun, C.; Luo, J.; Suib, S. L.; Hayashi, Y.; Matsumoto, H. *J. Catal.* **1998**, *178*, 372.

JP100346Q